High-Field EPR Study of Carotenoid and Chlorophyll Cation Radicals in Photosystem II

ARTICLE *in* THE JOURNAL OF PHYSICAL CHEMISTRY B · OCTOBER 2000

Impact Factor: 3.3 · DOI: 10.1021/jp002558z

6 AUTHORS, INCLUDING:

K. V. Lakshmi
Rensselaer Polytechnic Institute
78 PUBLICATIONS **2,409** CITATIONS
SEE PROFILE

Oleg G Poluektov
Argonne National Laboratory
86 PUBLICATIONS **1,410** CITATIONS
SEE PROFILE

Arlene M. Wagner
Argonne National Laboratory
13 PUBLICATIONS **114** CITATIONS
SEE PROFILE

Marion Charlotte Thurnauer
Argonne National Laboratory
148 PUBLICATIONS **6,292** CITATIONS
SEE PROFILE

THE JOURNAL OF PHYSICAL CHEMISTRY B

 VOLUME 104, NUMBER 45, NOVEMBER 16, 2000

LETTERS

High-Field EPR Study of Carotenoid and Chlorophyll Cation Radicals in Photosystem II

K. V. Lakshmi,[‡] Michael J. Reifler,[‡] Gary W. Brudvig,*[,‡] Oleg G. Poluektov,[†] Arlene M. Wagner,[†] and Marion C. Thurnauer*[,†]

Department of Chemistry, Yale University, P.O. Box 208107, New Haven, Connecticut 06520-8107, and Chemistry Department, Argonne National Laboratory, 9700 South Cass Avenue, Argonne, Illinois 60439

Received: July 19, 2000; In Final Form: September 19, 2000

In photosystem II (PS II), chlorophyll, β-carotene, and cytochrome b_{559} are alternate electron donors that may be involved in a photoprotection mechanism. The present study describes the use of high-field EPR spectroscopy to characterize the low-temperature photooxidation of Chl_Z and Car cofactors in PS II. The EPR signals of the individual species, previously not resolved at X-band frequency (9 GHz), are resolved at higher D-band frequency (130 GHz) in deuterated *Synechococcus lividus* PS II. Deuteration of PS II results in significant narrowing of the EPR lines, yielding well-resolved EPR spectra of the Car^+ and Chl_Z^+ radicals at 130 GHz. The g tensors of the individual species were determined by EPR spectral simulations. The g tensor determined for the Car^+ radical ($g_{xx} = 2.00335$, $g_{yy} = 2.00251$, $g_{zz} = 2.00227$) is similar to that previously observed for a canthaxanthin cation radical but with a slightly rhombic tensor. The Chl_Z^+ g tensor ($g_{xx} = 2.00312$, $g_{yy} = 2.00263$, $g_{zz} = 2.00202$) is similar to that of a chlorophyll *a* cation radical. This study shows that both the carotenoid and chlorophyll radicals are generated in PS II by illumination at temperatures from 6 to 190 K and that there is no interconversion of Car^+ and Chl_Z^+ radicals upon dark annealing at temperatures up to 160 K. This study also establishes the feasibility of using deuteration and high-field EPR to resolve previously unresolvable cofactor signals in PS II.

Introduction

Carotenoid and chlorophyll pigments assume several roles in natural photosynthesis. They participate in both singlet and triplet energy transfer as antenna and photoprotective pigments, respectively.[1−3] Carotenoids are also important as part of synthetically linked donor−acceptor macromolecules.[4,5] In these systems, they serve as "molecular wires" in photogenerated charge separation. This latter function is utilized as part of an alternate electron-transfer pathway in photosystem II (PS II).[6−10]

In the primary photoreaction of PS II, a donor chlorophyll undergoes excitation resulting in a series of short-lived charge-separated states that are stabilized by rapid electron transfer along a chain of donors and acceptors, culminating in the oxidation of water and reduction of a diffusible quinone. However, there exists a secondary electron-transfer pathway in PS II that involves cytochrome b_{559} (cyt b_{559}), a monomeric chlorophyll (Chl_Z), and a redox-active carotenoid (Car). In the event that electron transfer from the water-oxidizing center to the primary donor chlorophyll, P_{680}^+, is blocked, this alternate secondary electron-transfer pathway is in effect and P_{680}^+ radicals are quenched by electrons from Chl_Z, Car, and cyt b_{559}. It has been proposed that this secondary electron-transfer pathway is important to protect PS II from photodamage.[11−13]

* Authors to whom correspondence should be addressed. Gary W. Brudvig, Phone: (203) 432 5202. Fax: (203) 432 6144. E-mail: Gary.Brudvig@Yale.Edu. Marion C. Thurnauer, Phone: (630) 252 3570. Fax: (630) 252 4470. E-mail: mariont@anl.gov.
† Argonne National Laboratory.
‡ Yale University.

10.1021/jp002558z CCC: $19.00
Published on Web 10/21/2000

The presence of Car^+ and Chl_Z^+ radicals in PS II and the mechanistic aspects of the secondary electron-transfer pathway have been studied by optical and X-band EPR spectroscopy.[6−9] These studies have shown that illumination of samples below 60 K yields a mixture of Chl_Z^+ and Car^+ whereas illumination at higher temperatures yields predominantly Chl_Z^+ owing to the greater stability of Chl_Z^+ over Car^+. Although the Car^+ and Chl_Z^+ peaks are well resolved in the optical spectra (at 990 and 820 nm, respectively), quantitation of these centers is difficult due to an uncertainty in the extinction coefficients. At X-band EPR frequency, the Car^+ and Chl_Z^+ radicals exhibit a single unresolved peak. Studies of the relative yields and interconversion between the two radicals in PS II are based on small differences in the g values and line width changes at X-band EPR frequency.[6]

In the present study, we demonstrate that deuteration of PS II, combined with manganese depletion and illumination at low temperatures, results in resolved EPR spectra of the Car^+ and Chl_Z^+ radicals at 130 GHz. Spectral simulations of the experimental spectra establish the g tensors for Car^+ and Chl_Z^+. It is found that the Chl_Z^+ g tensor in the protein environment is similar to the tensor of a chlorophyll *a* cation radical measured in a frozen solution[14] ($g_{xx} = 2.00329$, $g_{yy} = 2.00275$, $g_{zz} = 2.00220$) and the Car^+ g tensor is slightly rhombic.

Materials and Methods

Sample Preparation. *Synechococcus lividus* cells were grown at 43 °C in deuterated Ac medium.[15,16] PS II core complexes were isolated from the deuterated cells on the basis of the procedure by Tang and Diner[17] with minor modifications. The sample was loaded onto the ion-exchange column in the absence of $MgSO_4$, and PS II was eluted with a 1-L gradient of 0−50 mM $MgSO_4$. SDS−polyacrylamide gels and densitometry scans showed a minor PS I contamination; P_{700}^+ was observed by EPR to be ∼14% of the maximal Chl_Z^+/Car^+ yield. Manganese depletion was performed by washing with 10 mM NH_2OH in the presence of 10 mM EDTA after which the sample was repeatedly washed with excess EDTA to remove free Mn^{2+} ions. Typically, EPR samples were prepared from deuterated Mn-depleted PS II samples at ∼8 mg Chl/mL in a buffer containing 20 mM $CaCl_2$, 5 mM $MgCl_2$, 50 mM MES, pH 6.0, with 20% (w/v) glycerol, 0.03% (w/v) β-DM, and 1 mM EDTA. The samples were preincubated with 200 μM ferricyanide in the dark at 0 °C to completely oxidize cyt b_{559} before loading into 0.45 mm quartz capillaries.

D-Band EPR Spectroscopy. High-field EPR spectra were obtained on a home-built D-band (130 GHz/4.5 T) continuous wave/pulsed instrument. The microwave bridge was constructed by Dr. V. N. Krymov (HF EPR Instruments, Inc.). The bridge consists of two independent channels driven by a frequency-fixed free-running oscillator. Each channel contains a linear combination of IMPATT amplifiers. The microwave power from each channel is combined by a directional coupler and directed through the circulator to a single-mode TE_{011} cavity. The maximum output power of the circulator in the pulsed mode is 125 mW (34 ns $\pi/2$ pulses) and 3.4 mW in the *cw* mode. The cavity has several slits to allow for optical excitation and field modulation. For light excitation, an optical parametric oscillator (Opotek) pumped by a Nd:YAG laser (Quantel) is used and the output of the laser is coupled to a fiber optic which delivers light to the cavity (2 mJ per pulse). The cavity temperature is regulated by an Oxford temperature controller (ITC 503) coupled to an Oxford continuous flow cryostat (CF 1200).

Deuterated Mn-depleted PS II samples in 0.45 mm i.d. quartz tubes were placed in the cavity and frozen in the dark in the presence of the magnetic field. The samples were illuminated at the indicated temperatures inside the EPR cavity for 15 min with laser flashes at 550 nm with a repetition rate of 10 Hz. To minimize rapid-passage effects and obtain better resolution, spectra were recorded at higher temperature (70 K) with the microwave power attenuation set at 45 dB unless otherwise noted. Magnetic field modulation was set at 1.5 G. Typically, 10−20 scans were averaged for each dark and illuminated spectrum and all spectra were acquired in the dark.

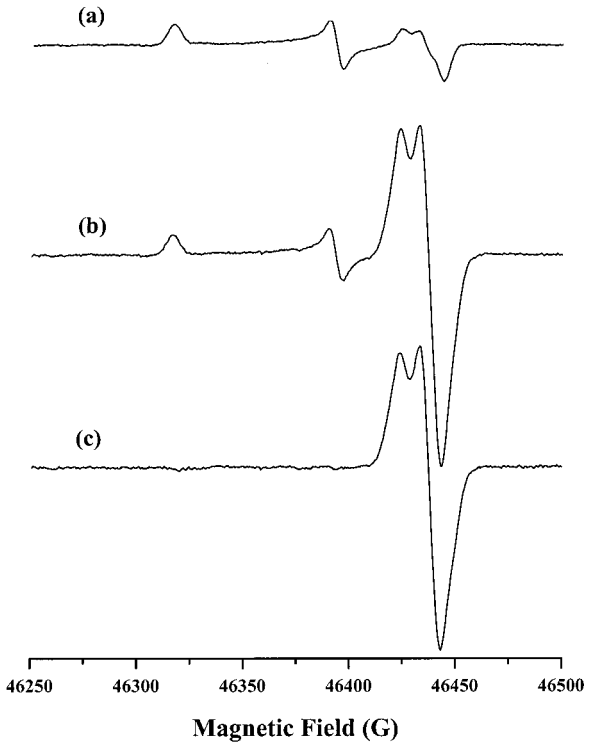

Figure 1. D-band EPR spectra of deuterated Mn-depleted *S. lividus* PS II. (a) Background signals recorded in the dark from stable tyrosine-D radicals in PS II[19] and chemically oxidized P_{700}^+ radicals[21,20] from the small PS I contamination. (b) Signals recorded after illumination at 30 K. (c) Light-minus-dark difference spectrum (b − a) showing signals from the Car^+ and Chl_Z^+ radicals. The illuminated and dark spectra were acquired at 30 K with a modulation amplitude of 1.5 G and microwave power of 0.1 μW.

Simulations were performed with Bruker simulation software (Simfonia). The starting g values were taken from high field studies of Car^+ and Chl a^+ by Konovalova et al.[18] and Bratt et al.,[14] respectively. The g values, width of the canonical components, and the relative contribution of the two radical species were adjusted to obtain a best fit to the composite spectra.

Results

Figure 1a−c shows D-band EPR spectra of deuterated Mn-depleted *S. lividus* PS II. As can be seen in the spectrum in Figure 1a, background signals from dark-stable tyrosine-D radicals in PS II[19] and chemically oxidized P_{700}^+ signals[20,21] from the small PS I contamination are present in the dark. Upon continuous illumination at 30 K (Figure 1b), additional signals, that we attribute to the Car^+ and Chl_Z^+ radicals, appear in the high-field region of the spectrum. Signals solely from the superimposed radicals are obtained in the light-minus-dark difference spectrum shown in Figure 1c.

Figure 2 shows experimental light-minus-dark difference spectra and spectral simulations of protonated and deuterated Mn-depleted *S. lividus* PS II illuminated at different tempera-

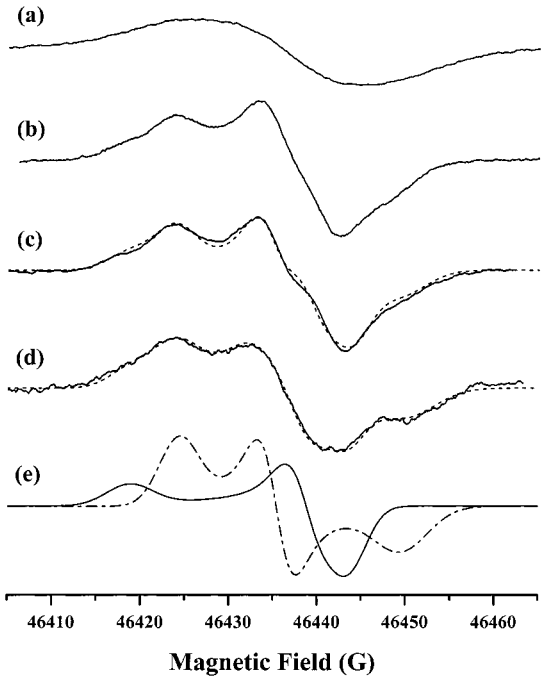

Figure 2. Experimental difference spectra and spectral simulations of protonated and deuterated Mn-depleted *S. lividus* PS II illuminated at different temperatures. (a) Experimental spectrum of protonated PS II obtained upon illumination at 30 K. (b, c, and d) Experimental light-minus-dark difference spectra (solid lines) of Mn-depleted deuterated PS II obtained after illumination at 30, 6, and 190 K, respectively. Also shown as dotted lines are the composite spectral simulations obtained by the addition of the Car^+ and Chl_Z^+ spectra in varying proportions. (e) Individual simulated EPR signals from the Car^+ (solid line) and Chl_Z^+ (dashed/dotted line) cation radicals that contribute to the composite simulated spectra shown in (c) and (d). The experimental spectra were acquired with a modulation amplitude of 1.5 G and microwave power of 0.05 μW. The spectra in (a) and (b) were acquired at 30 K; the spectrum in (b) is slightly broadened due to saturation effects. The spectra in (c) and (d) were acquired at 70 K.

tures. Figure 2a,b shows spectra of protonated and deuterated *S. lividus* PS II under continuous illumination at 30 K, respectively. Figure 2c,d shows experimental spectra (solid lines) of deuterated *S. lividus* PS II obtained after continuous illumination at 6 and 190 K, respectively. The spectra shown in Figure 2c,d were recorded at 70 K following the illuminations, but the spectrum of the sample illuminated at 6 K and measured at 70 K (Figure 2c) is equivalent to that of a sample illuminated and measured at 30 K (Figure 2b). As can be seen in the experimental spectra, the line shapes are different in the 6 K-illuminated and 190 K-illuminated difference spectra. Also shown as dotted lines are the composite spectral simulations obtained by the addition of the Car^+ and Chl_Z^+ line shapes in varying proportions. Figure 2e shows individual simulated EPR signals from the Car^+ and Chl_Z^+ radicals that contribute to the composite simulated spectra shown in Figure 2c,d.

As can be qualitatively seen in the experimental spectra in Figure 2c,d, 190 K illumination of deuterated Mn-depleted PS II yields a greater proportion of Chl_Z^+ relative to Car^+ than does illumination at 6 K. The g tensors and relative yields of Car^+ and Chl_Z^+ radicals used to simulate the experimental 6 K-illuminated, 85 K-illuminated, and 190 K-illuminated spectra (spectrum not shown for the 85 K-illuminated sample) are summarized in Table 1. As can be seen, the Car^+ and Chl_Z^+ g tensors used in all the simulations are within 0.00004 of each other. The origin of slight deviations could be due to a distortion of the EPR line shape owing to saturation and rapid-passage effects.[22,23]

TABLE 1: Parameters Used To Simulate the Experimental Spectra Shown in Figures 2c,d

illumination temperature	g tensor[a] Car^+	g tensor[a] Chl_Z^+	Car^+ yield[b]	Chl_Z^+ yield[b]
6 K	$g_{xx} = 2.00335$ $g_{yy} = 2.00249$ $g_{zz} = 2.00227$	$g_{xx} = 2.00311$ $g_{yy} = 2.00262$ $g_{zz} = 2.00201$	46%	54%
85 K	$g_{xx} = 2.00335$ $g_{yy} = 2.00251$ $g_{zz} = 2.00227$	$g_{xx} = 2.00312$ $g_{yy} = 2.00264$ $g_{zz} = 2.00204$	43%	57%
190 K	$g_{xx} = 2.00335$ $g_{yy} = 2.00253$ $g_{zz} = 2.00228$	$g_{xx} = 2.00313$ $g_{yy} = 2.00265$ $g_{zz} = 2.00201$	32%	68%

[a] The line widths used for the Car^+ and Chl_Z^+ simulations are in the range of 4.0 and 5.0 G, respectively, with a 20% variation in the g_{xx}, g_{yy}, and g_{zz} components. [b] The data are normalized to a total radical yield of 100% for each illumination temperature. The total radical yield decreases progressively as the illumination temperature is increased.[9]

Relative decay of the Car^+ and Chl_Z^+ radical signals with dark annealing at higher temperatures was also studied. High-field EPR spectra of a sample illuminated at 6 K for 10 min followed by dark annealing at 85 and 160 K for 60 min (spectra not shown) indicate a decrease in both the Car^+ and Chl_Z^+ signals but do not indicate an interconversion between the two populations.

Discussion

The present study describes the low-temperature photooxidation of Chl_Z and Car cofactors in PS II. The EPR signals of the individual species, previously not resolved at X-band frequency (9 GHz), are resolved at D-band frequency (130 GHz) in deuterated Mn-depleted *S. lividus* PS II. Deuteration of PS II results in significant narrowing of the EPR lines at 130 GHz in comparison to the spectrum obtained from protonated PS II at 130 GHz and canthaxanthin radicals at 327 GHz.[18] The g tensors of the individual Car^+ and Chl_Z^+ species are accurately reproduced by EPR spectral simulations. The g values determined for the Car^+ radical are close to those previously observed for canthaxanthin[18] ($g_{para} = 2.0032$ and $g_{perp} = 2.0023$) but with a slightly rhombic g tensor (Table 1).

The Chl_Z^+ g tensor (Table 1) is close to that of a chlorophyll *a* cation radical in a frozen methylene chloride solution.[14] Although the g values for Chl_Z^+ in this study are lower than the g values for Chl a^+ in solution, the ($g_{xx} - g_{zz}$) and ($g_{yy} - g_{zz}$) values are similar. This could be due to a systematic error in the absolute measurement of g tensors. To avoid a systematic error in this study, the g values for Car^+ and Chl_Z^+ are calibrated relative to the g_{yy} component of the P_{700}^+ signal in the dark spectrum ($g_{yy} = 2.00264$).[21] The high-field (330 GHz) EPR spectrum of Chl a^+ induced by low-temperature illumination of a spinach PS II membrane sample has been reported previously,[24] although the value of $\Delta g = (g_{zz} - g_{xx})$ obtained in this study ($\Delta g = 0.00091$) is smaller than we observe for Chl_Z^+ ($\Delta g = 0.00110$). It is interesting to note that the value of Δg that we have determined for Chl_Z^+ in PS II, while similar to the Δg for isolated Chl a^+ in a frozen solution ($\Delta g = 0.00109$),[14] is larger than the Δg for P_{700}^+ in PS I ($\Delta g = 0.00091$).[21] The Δg for Chl_Z^+ in PS II and Chl a^+ in solution are representative of a monomeric chlorophyll cation radical. The smaller Δg for P_{700}^+ may reflect some delocalization of the spin density over the two chlorophyll rings in the P_{700} special pair.[14]

The results of this study support the hypothesis that both chlorophyll and carotenoid are involved in the secondary

electron-transfer pathway in PS II. The spectral simulations provide the relative yields of the two radicals at different illumination temperatures. Previous studies have indicated that 77 K illumination gives rise to the Car^+ radical while illumination at 200 K gives rise to Chl_Z^+.[7] More recently, Rutherford and co-workers have reported that illumination at 20 K results in near stoichiometric yields of Car^+, which has been the basis for spin−echo modulation studies.[6,25] However, the present study indicates that, although greater signal yields of Chl_Z^+ are obtained with illumination at 190 K, there is a significant yield of Car^+ radicals in a Mn-depleted PS II sample illuminated at 6, 85, or 190 K. The relative yields of Car^+ and Chl_Z^+ radicals obtained with illumination at different temperatures and EPR spectral simulations are in agreement with recent results obtained with optical spectroscopy.[9]

Previous studies by Hanley et al.[6] have reported that continuous illumination at 20 K followed by dark annealing at 120 K results in a Car^+-to-Chl_Z^+ conversion. High-field EPR spectra of Mn-depleted PS II dark annealed at 85 and 160 K after preillumination at 6 K do not indicate an interconversion between the Car^+ and Chl_Z^+ radical species. Rather a decay of both the Car^+ and Chl_Z^+ signals is observed in the dark at 85 and 160 K. Independent optical and X-band EPR data[9] reproduce the same trend following dark annealing steps ranging from 30 to 120 K and show a decay of Car^+ and Chl_Z^+ by charge recombination with Q_A^- without an interconversion of Car^+ and Chl_Z^+ in cyanobacterial PS II samples.

Acknowledgment. Work at ANL was supported by the U.S. Department of Energy, Office of Basic Energy Sciences, Division of Chemical Sciences, under contract W-31-109-Eng-38. Work at Yale University was supported by the NIH (GM32715). We acknowledge S. Schlesselman at ANL for technical support.

References and Notes

(1) Lawlor, D. W. *Photosynthesis: Metabolism, Control and Physiology*; Wiley: New York, 1987.

(2) Goodwin, T. W. *The Biochemistry of the Carotenoids: Plants*; Chapman and Hall: London, 1980.

(3) Cogdell, R. J.; Frank, H. A. *Biochim. Biophys. Acta* **1987**, *895*, 63−79.

(4) Kuciauskas, D.; Liddell, P. A.; Lin, S.; Stone, S. G.; Moore, A. L.; Moore, T. A.; Gust, D. *J. Phys. Chem. B* **2000**, *104*, 4307−4321.

(5) Gust, D.; Moore, T. A.; Moore, A. L. *Z. Phys. Chem.* **1999**, *213*, 149−155.

(6) Hanley, J.; Deligiannakis, Y.; Pascal, A.; Faller, P.; Rutherford, A. W. *Biochemistry* **1999**, *38*, 8189−8195.

(7) Noguchi, T.; Mitsuka, T.; Inoue, Y. *FEBS Lett.* **1994**, *356*, 179−182.

(8) Schenck, C.; Diner, B. A.; Mathis, P.; Satoh, K. *Biochim. Biophys. Acta* **1982**, *680*, 216−227.

(9) Tracewell, C. A.; Cua, A.; Stewart, D. H.; Bocian, D. F.; Brudvig, G. W. *Biochemistry*, submitted.

(10) Vrettos, J. S.; Stewart, D. H.; de Paula, J. C.; Brudvig, G. W. *J. Phys. Chem. B* **1999**, *103*, 6403−6406.

(11) Schweitzer, R. H.; Brudvig, G. W. *Biochemistry* **1997**, *36*, 11351−11359.

(12) Stewart, D. H.; Brudvig, G. W. *Biochim. Biophys. Acta* **1998**, *1367*, 63−87.

(13) Thompson, L. K.; Brudvig, G. W. *Biochemistry* **1988**, *27*, 6653−6658.

(14) Bratt, P. J.; Poluektov, O.; Thurnauer, M. C.; Krzystek, J.; Brunel, L.-C.; Schrier, J.; Hsiao, Y.-W.; Zerner, M.; Angerhofer, A. *J. Phys. Chem. B* **2000**, *104*, 6973−6977.

(15) Kratz, W.; Myer, J. *J. Botany* **1955**, *42*, 282−287.

(16) Daboll, H. F.; Crespi, H. J.; Katz, J. J. *Biotechnol. Bioeng.* **1962**, *4*, 218−297.

(17) Tang, X.-S.; Diner, B. A. *Biochemistry* **1994**, *33*, 4594−4603.

(18) Konovalova, T. A.; Krzystek, J.; Bratt, P. J.; van Tol, J.; Brunel, L. C.; Kispert, L. D. *J. Phys. Chem. B* **1999**, *103*, 5782−5786.

(19) Un, S.; Atta, M.; Fontecave, M.; Rutherford, A. W. *J. Am. Chem. Soc.* **1995**, *117*, 10713−10719.

(20) Prisner, T. F.; McDermott, A. E.; Un, S.; Norris, J. R.; Thurnauer, M. C.; Griffin, R. G. *Proc. Natl. Acad. Sci. U.S.A.* **1993**, *90*, 9485−9488.

(21) Bratt, P. J.; Rohrer, M.; Krzystek, J.; Evans, M. C. W.; Brunel, L.-C.; Angerhofer, A. *J. Phys. Chem. B* **1997**, *101*, 9686−9689.

(22) Krinichni, V. I.; Grinberg, O. Y.; Dubinski, A. A.; Lifshits, B. A.; Bobrov, Y. A.; Lebedev, Y. S. *Biofizika (in Russian)* **1987**, *32*, 534−535.

(23) Grinberg, O. Y. High g-Resolution EPR Spectroscopy. Method and Applications. Thesis Dr. Science, Russian Academy of Sciences, 1988.

(24) MacMillan, F.; Rohrer, M.; Krzystek, J.; Brunel, L.-C.; Rutherford, A. W. In *Photosynthesis: Mechanisms and Effects*; Garab, G., Ed.; Kluwer Academic Publishers: Dordrecht, 1998; Vol. 2, pp 715−718.

(25) Deligiannakis, Y.; Hanley, J.; Rutherford, A. W. *J. Am. Chem. Soc.* **2000**, *122*, 400−401.